



ELSEVIER

Available online at [www.sciencedirect.com](http://www.sciencedirect.com)

SCIENCE @ DIRECT®

**Nonlinear  
Analysis**

Real World Applications

Nonlinear Analysis: Real World Applications 6 (2005) 705–730

[www.elsevier.com/locate/na](http://www.elsevier.com/locate/na)

# Describing space-time patterns in aquatic ecology using IBMs and scaling and multi-scaling approaches

Sami Souissi<sup>a,\*</sup>, Laurent Seuront<sup>a,b</sup>, François G. Schmitt<sup>a</sup>,  
Vincent Ginot<sup>c</sup>

<sup>a</sup>*Ecosystem Complexity Research Group, Station Marine de Wimereux, Université des Sciences et Technologies de Lille, CNRS - UMR 8013 ELICO, 28 avenue Foch, BP 80, F-62930 Wimereux, France*

<sup>b</sup>*School of Biological Sciences, Flinders University, GPO Box 2100, Adelaide SA 5001, Australia*

<sup>c</sup>*INRA, Unité de biométrie, Domaine St-Paul, 84914 Avignon, Cedex 9, France*

## Abstract

In this paper a new simulation platform, “*Mobidyc*”, dedicated to non-computer expert end-users, is used to illustrate the advantages of such platforms for simulating population dynamics in space and time. Using dedicated and open-source platforms probably represents a necessary step to guarantee the readability and comparison between models and/or scenarios. The “*Mobidyc*” platform is specifically dedicated to population dynamics with 2D-discrete spatial representation. We show first how to build easily stage-structured population dynamics models, on the basis of an experimental parameterization of the population dynamic of the copepod *Eurytemora affinis*, the most dominant species in estuaries of the Northern hemisphere. We subsequently focus on the role of spatial representation and the possible sources of heterogeneities in copepod populations. The sources generating patterns in our examples are strictly endogenous to the population and individual characteristics. They are generated by the random walk of individual at local scale and the demographic processes (birth, metamorphosis and mortality) at the population scale in the absence of any externally imposed pattern.

The large spatio-temporal data sets of abundances of total population are analysed statistically. Spatial and temporal patterns are investigated using models and data analysis techniques initially developed in the fields of turbulence and nonlinear physics (e.g. scaling and multi-scaling approaches

\*Corresponding author. Tel.: +33 321 992 908; fax: +33 321 992 901.

E-mail address: [sami.souissi@univ-lille1.fr](mailto:sami.souissi@univ-lille1.fr) (S. Souissi).

for data analysis and stochastic simulation). Finally, the role of simulation tools for theoretical studies is discussed in this paper.

© 2005 Elsevier Ltd. All rights reserved.

*Keywords:* Individual-based models (IBM); Copepod population; Spatial patterns; Scaling and multi-scaling

---

## 1. Introduction

Over the last decade, the modelling of biological systems has undergone great development resulting in many improvements over a wide range of scientific disciplines. It is clear that increases in computer power and modelling tool and simulator development are the major determining factors of this change [7,20]. However, the complexity of biological systems, and gaps in the fundamental understanding of the identification of some complex behavioural responses of individuals or populations has handicapped the development of coherent and comparable models.

In ecology many processes can be assimilated to discrete events, thus their representation by continuous mathematical functions may be nothing more than a phenomenological description of the net result of many processes, which are poorly understood or even not understood [19]. We will thus refer to the definition of individual-based models (referred to as IBMs hereafter) relying upon the recent development of models based on object-oriented computer languages and associated tools and simulators [36]. According to these authors, IBMs should include discrete individuals with their complete life cycles, as well as differences between individuals and the dynamics of the resources (in general with spatial heterogeneity) upon which the individuals compete. This approach makes more realistic assumptions and allows for the representation of the differences between individuals and the main processes at the individual scale. This framework is very close to the biologist point of view, the representation of functional responses (i.e. mathematical models) allowing the simulation of mean behaviour of the population is no longer made, but the emerging properties at the population level resulted from the diversity of individual trajectories and their adaptation capabilities in the simulation. When individuals differ in their abilities to acquire and/or to compete for resources, populations are able to persist at much smaller population sizes [17]. The properties simulated at larger scales (population scale or larger spatial domains) are not strictly deterministic and are called “emerging properties” [27]. Multi-agent systems (MAS), which are a collection of independent agents interacting via discrete events [24], subsequently provide an adequate framework for developing IBMs fitted to the present challenge of modelling copepod individuals, populations and food-webs [33].

Although IBMs offer a great potential for challenging ecological studies, this potential is still far from being fully exploited [12]. Consequently more “experiments” using IBMs should be conducted to try to relate them more directly to theory. The first applications tried to compare IBM representations to their representative analytical formulation [38,34,4]. Even if these IBM formulations were close to the analytical model at the population level, it has been shown that the outcome of IBMs can or cannot be comparable to the results provided by more standard modelling approaches. This is another demonstration of the

potentials of IBMs to provide new insights into a priori known dynamics of some systems and particularly for patterns in both space and time.

The development and use of IBMs in both aquatic and terrestrial ecology is continuously increasing [12]. However, several authors recognize the necessity of improving computer implementation and reproducibility of models [11]. A significant effort has thus been made on the “technical” aspects of modelling by proposing platforms and simulators dedicated for IBMs [20]. All these recent papers have aimed at improving the great potential of IBMs in contributing significantly to render this approach of modelling more popular [12,11]. However, this progress cannot be achieved without paying a particular attention to the way to decide on model structure and to make the model readable and testable. Some authors focused on these questions and suggested some concepts to improve IBMs, as the use of (i) complex adaptive systems concepts as a theoretical foundation for IBMs [27], (ii) component programming and dedicated platforms to simplify IBMs conception and enhance their flexibility [11], and (iii) pattern-oriented modelling [13]. Nonetheless all these aspects of improving IBMs development could be incomplete if we do not try to relate them more directly to theory [33]. In particular, the concepts of emergence, adaptive traits, and fitness are critical for devising theory of how individual traits explain system behaviours [14]. We show in this paper that the end-user platforms (e.g. *MobidyC*) and associated tools can significantly contribute to developing a common framework for linking IBMs to theory. These tools contributed to make IBMs more popular and more accessible to ecologists. It is thus possible to focus on more general questions because the model structure and its development are no longer the main question. In this paper we focus on the properties of spatio-temporal patterns generated by a stochastic IBM. It is a new way of analysing the emerging properties of some classes of IBMs towards linking them to more analytical and/or statistical theory.

The number of biological and ecological studies focusing on the spatio-temporal patterns emerging from IBMs is now subsequently and naturally increasing (e.g. [18,23,28]). However, we are not aware of any attempt to quantify the structure of the emerging patterns in space and/or in time. It is nevertheless a critical issue in ecology, and more specifically in aquatic ecology, where two fundamental and interconnected themes are (i) the development and maintenance of spatial and temporal patterns, and (ii) the consequences of the patterns for the dynamics of populations and ecosystems. In particular, zooplankton organisms exhibit patchiness over a broad range of spatial and temporal scales, i.e. from micrometers to hundreds of meters and from seconds to months [22,8]. The scale issue is particularly critical in the framework of IBMs as many microscale processes (e.g. feeding and mating behaviours) relevant at the individual levels are likely to affect the bioenergetics of individual organisms and ultimately the population dynamics of zooplankton. In addition, because patterns of zooplankton spatial variability and generating processes are scale-dependent [35,1,29], zooplankton structure must be investigated using scaling and/or multi-scaling approaches. This consists in considering first the spatial distribution of the population: the fractal analysis of the support of this population is a useful tool that describes its heterogeneity, and its patterns, at all scales. Such approach seems very appropriate for multi-scale patterns, which is the case here for the simulation analysed. On the other hand, the sharp fluctuations—called intermittencies—corresponding to the variable levels in total population per cell, are characterized using a multi-scaling framework,

where each intensity is associated to a given fractal dimension, hence the name multifractal.

In this context, the objective of this paper is to combine the use of IBMs and scaling and multi-scaling approaches to characterize qualitatively and quantitatively emerging space-time patterns. We use a recently developed platform dedicated to end-users and adapted to make numerical experiments, leading us to the step of analysis of simulation. After an introduction of the main characteristics of the platform, it will be applied to a population dynamics model calibrated for *Eurytemora affinis*, the most abundant species of copepod in estuaries of the Northern Hemisphere. This species has been specifically chosen because of (i) its ecological relevance and (ii) our extensive knowledge of its biological properties at the individual level [6] that allows the elaboration of a realistic model. We subsequently introduce the scaling and multi-scaling framework, and analyse the emerging space-time patterns of the simulated population, with a special focus on the effects of the size of the spatial domain on model outcome.

## 2. Development of the model

### 2.1. Use of “Mobydyc” platform

The “Mobydyc” platform is dedicated to non-computer expert end-users, with a flexible architecture based on the use of MAS paradigm, which defines agents as autonomous objects that perceive and react to their environment. *Mobydyc* focuses more on what each agent does than on what it actually is and provides three kinds of agents: (i) Animats (moving agent) that represent the typical individuals, (ii) Cells that represent a discretization of the space, and, (iii) Non-located agents that are optional and may provide general scenarios for all other agents or compute the results that the user wishes to save.

The advantage of this approach is that all the different elementary tasks that form the behaviour of individuals can be clustered into a low number of classes of activities, e.g. locate, select, translate, compute, end, and workflow control [11].

### 2.2. Life cycle representation and model architecture

From an individual point of view, each individual of a copepod population has to follow the schematic template shown in Fig. 1. Most copepods exhibit a clear sexual dimorphism with only one reproductive stage (adults: C6). After copulation each mature female can produce a certain number of eggs. Between embryonic and mature stages each individual should pass successively through the six larval (naupliar) stages and the five juvenile (copepodite) stages. In order to simplify the copepod life cycle, the naupliar stages were aggregated into two groups as proposed by Souissi and Ban [32] whereas the copepodite stages were represented in detail. Moreover, females and males are separated since the last copepodite stage (C5), because their development is different.

Each individual is represented by an animat where in its basic form contains three attributes: age, location, and number, and one predefined task corresponding to ageing of individuals (grow older). In this model the attribute number is set to one to represent an

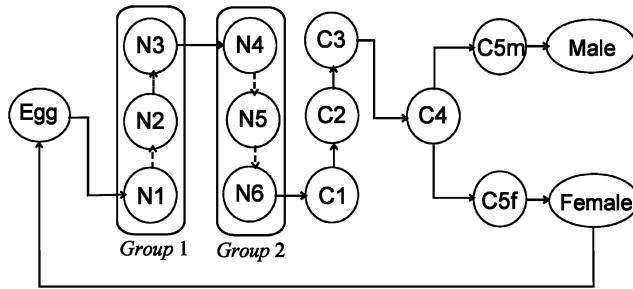


Fig. 1. Schematic representation of life cycle of the copepod *Eurytemora affinis* with aggregation of the larval stages into two groups: N1–N3 and N4–N6. Sexes are separated at the last juvenile stage (C5). A “Mobydyc” agent containing a dictionary of attributes and an ordered dictionary of tasks represents each stage.

Table 1  
List of attributes used to define the life cycle of the copepod *Eurytemora affinis*

Attribute	Owner	Definition
Age	All stages	Age (days)
Location	All stages	Position in the grid of cells
Number	All stages	Number of individuals per agent
rand	All stages	Intermediate, used to assign a random real between 0 and 1
state	All stages	Intermediate, used to define the state of survival
pSurv	All stages	Probability of survival in the stage
meanDuration	All stages	Mean stage duration for stages Egg to C5, and life span in stage adult (C6)
alpha	All stages	Parameter for the variability around mean stage duration
minDuration	All stages	Intermediate, used to compute the minimum stage duration
maxDuration	All stages	Intermediate, used to compute the maximum stage duration
duration	All stages	Stage duration
stateSex	C4	Intermediate, used to define the type of sex in the stage C5
pFemale	C4	Sex-ratio of the population (proportion of females)
fecund	Female	Fecundity

individual; however, for other models the number can be an integer (i.e. group of individuals) or a real number (i.e. concentration of a subpopulation). The complete list of attributes needed to complete the definition of the model is shown in Table 1.

### 3. Application to *Eurytemora affinis* population

Among estuarine copepod species *E. affinis* is dominant in the temperate estuaries of the Northern Hemisphere [16,2,10] and its spatial repartition is generally restricted to the low-salinity zone. Several experimental studies were carried out in the laboratory in order to study the development of the population of this species under several conditions of food, temperature and salinity [6]. This species offers a good example for estimating the parameter values and then get realistic representation of the development of a population dynamics model. However, for the sake of simplicity, the simulation will be done under constant and optimal conditions of development corresponding to the temperature of 15 °C.

Table 2

Definition of the tasks used to develop the life cycle of the copepod *Eurytemora affinis*

Agent task	Definition	Type	Setting
Grow older	Compute the age of the agent	Predefined	my_age := my_age + simulator_timeStep
StateSurvive	Determine the state of the agent for survival	Predefined (ModifyAttributes)	my_rand := Random_real[0, 1] my_state := my_pSurv - my_rand
CondMortality	Conditional mortality	Predefined	if my_state < 0 then I am dead
TempDuration	Computation of the duration in each stage	Predefined (ModifyAttributes)	my_MinDuration := ((1 - my_alpha) * my_MeanDuration) my_MaxDuration := ((1 + my_alpha) * my_MeanDuration) my_duration := Random real [my_MinDuration,my_MaxDuration]
Hatching/ Moulting	Transfer from one stage to the next one	Predefined (Metamorphosis)	If my_age > my_duration
DefineSex	Define the sex of agent after moulting in the stage C4	Predefined (ModifyAttributes)	my_rand := Random_real[0, 1] my_stateSex := my_pFemale - my_rand
MoultingM/ MoultingF	Transfer from C4 to C5m/ from C4 to C5f	Predefined (Metamorphosis)	If (my_stateSex < 0) AND (my_age > my_duration)
Reproduction	Reproduction of females into eggs	Predefined (Reproduction)	/ ((my_stateSex >= 0) AND (my_age > my_duration)) Number of offsprings per individual equal to my_fecund

Note: The predefined task ‘ModifyAttributes’ is very useful for developing several models as the example shown here as it is specifically designed to deal with mathematical calculations involving agent attributes.

Table 2 shows the definition and the settings of the different tasks used in this model. The survival of any individual for a time step (here 0.25 day) is given by the sign of its state attribute (difference between *pSurv* and a random number between 0 and 1), i.e. for a high value of survival, the probability of obtaining a negative state is very low. As a consequence, the individual has a larger probability of surviving than dying during the simulation, and these rules (and may be others) are parameterized in the predefined task of mortality. Most agent behaviours require a computation of mathematical relations to update their attribute values. In *MobidyC*, this is done through the task “ModifyAttributes”. An example of its use is illustrated in Fig. 2 with the setting of the copepod duration in a stage. The stage duration for each individual is obtained by drawing a random real number between the minimal (i.e. the fastest individual) and maximal (i.e. the slowest individual) stage duration. The attributes “MeanDuration” and “alpha” are used to compute the previous limit of the possible values of stage duration.

### 3.1. Model parameterization and simulation without spatial representation

The biological trajectory shown in Fig. 1 was studied for several individuals under controlled and optimal conditions (abundant food and 15 °C). These experiments allowed to estimate the values of attributes “MeanDuration” and “alpha” for all developmental stages (Table 3). A clear difference on rate of development is observed between males and females in the last juvenile stage (C5). Females require the double time of males before moulting to the final adult stage (Table 3). This difference in physiology between sexes justifies the schematic template used in our model (Fig. 1). In order to complete the parameterization of the model a 1:1 sex-ratio is adopted (“pFemale” = 0.5). The same procedure used for survival is applied to determine randomly whether the individual in stage C4 will moult into C5f or C5m. Finally a constant fecundity rate is considered for females (5 eggs per female every time step) and reproduction starts after an observed delay of 2 days.

Before studying spatial patterns a first simulation without spatial representation is necessary. Starting with 50 males and 50 females, the detailed results of five runs of this

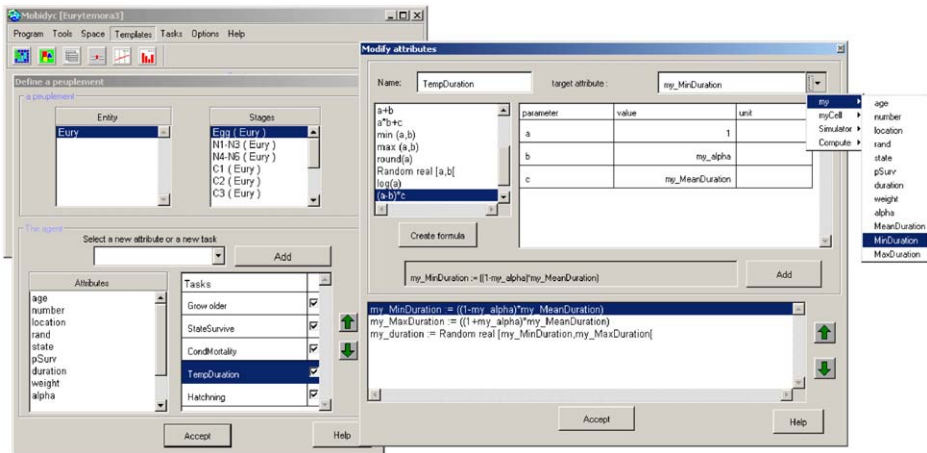


Fig. 2. Snapshot of the commonly used task “*ModifyAttributes*” to compute the stage duration (here embryonic development time) of an individual. The mathematical expression can be chosen from the list on the left or can be created using simple mathematical grammar syntax. A parameter value can be constant (fixed numerical value), an attribute value, or a function of an attribute value. For an animat, expressions can involve attributes of the running animat (i.e., *my\_duration*), of its cell (*myCell\_attributeName*), of one of the simulator characteristics (i.e., *Simulator\_timeStep*), or of any non-located agent. One task using “*ModifyAttributes*” can contain a series of mathematical instructions. The window in the second plane is used to define the community from the principal menu of “*Mobydyc*” interface, which is shown in the third plane.

Table 3  
Parameter values used in the simulations

Stages	Mean Duration (days)	alpha	pSurv
Egg	1.00	0.10	0.98
N1–N3	3.35	0.10	0.96
N4–N6	5.00	0.20	0.96
C1	4.50	0.30	0.98
C2	3.90	0.20	0.98
C3	3.40	0.40	0.98
C4	2.70	0.40	0.98
C5m	3.20	0.25	0.98
C5f	6.30	0.25	0.98
Male	32.20	0.20	0.98
Female	28.10	0.20	0.98

simulation are shown in Fig. 3. The model correctly simulates the succession of the developmental stages with respect to their stage durations (see discontinuous line in Fig. 3) and other demographic parameters such as fecundity and survival. The stochastic representation of the stage survivals (Table 2) shows the visible differences between the five runs realized with the same set of parameters (different curves in Fig. 3).

For the next sections the total abundance of the population will be considered as a synthetic descriptor for studying spatial patterns. The temporal pattern of this descriptor shows a

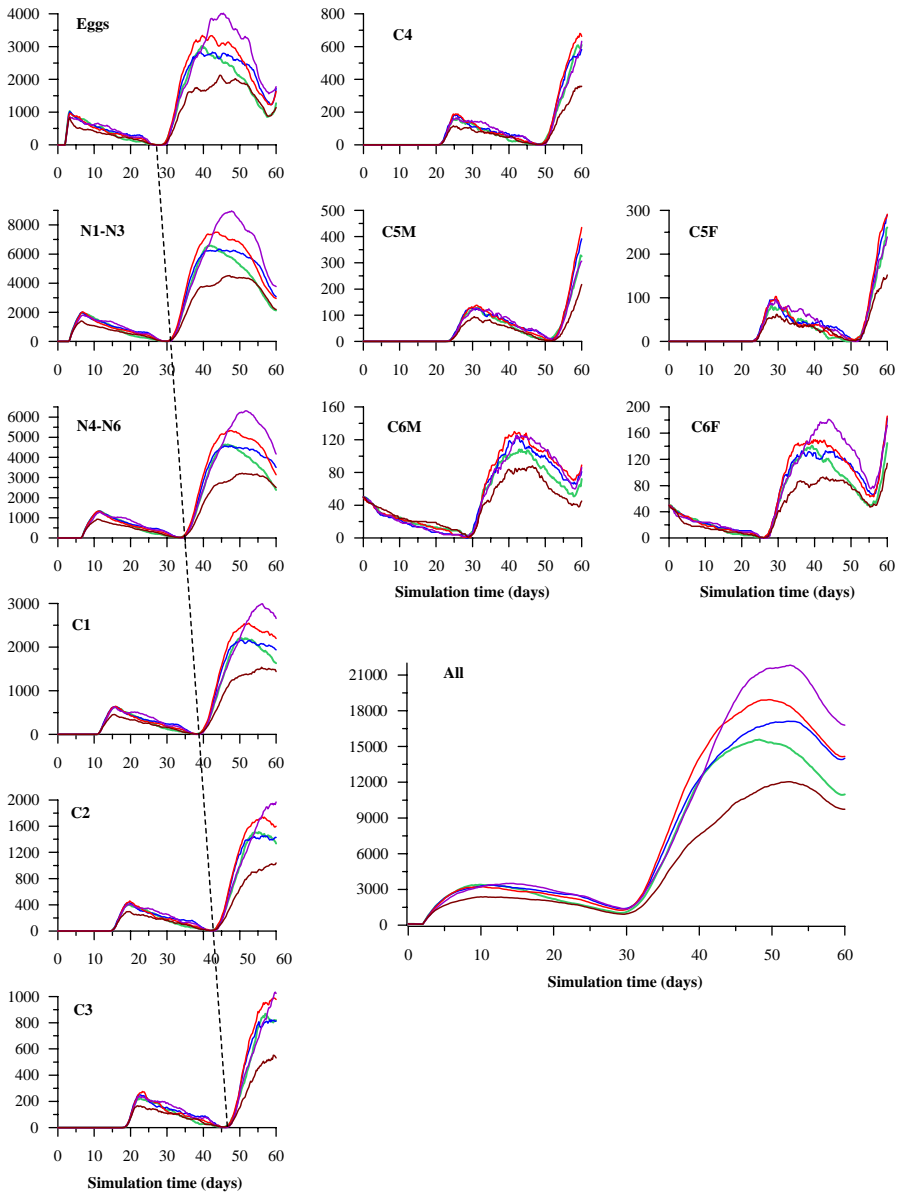


Fig. 3. Simulation of the development of the population of *Eurytemora affinis* during 2 months under constant temperature (15 °C) and without spatial representation. Five runs (represented with different colours) are realized with the same initial conditions of a mixture of 100 adults with a sex-ratio 1:1. Time evolution of each stage and for the complete population are shown. The discontinuous line shows the progression of a cohort development.

development of two generations of the copepod *E. affinis*. The growth of the population during the second generation is due to the high fecundity (constant) and also due to high values of probabilities of survival arbitrary used in this simulation (Table 3). We will mainly

focus hereafter on simulation times multiple of 10 days. These discrete values correspond to typical moments of the dynamics of this species during two generations.

### 3.2. Simulation with spatial representation

*Modelling behavioural scenarios of individuals.* An open grid of square cells where each cell has 8 neighbours represents space. Then a predefined task of moving is added and parameterized for all stages (excepting eggs). After each time step, individuals move to a cell randomly selected from its neighbourhood. In order to introduce a difference in motion between larval and later stages, the neighbourhood is set to one and two cells for larval and later stages, respectively.

*Using “primitives” and the “batch” mode to perform “numerical experiments”.* A default cell (spatial agent) contains two attributes only: location (cell position) and edge, which is a binary attribute, set to one for all boundary cells of the grid. But there is no boundaries here, as you use an open (i.e. torus) grid. In order to obtain spatio-temporal patterns of total density of the population a computation of the value of this descriptor in each cell and for each time step is necessary. The number of individuals in each cell was stored in list attribute (vector added by the user) by using the user-defined task “*CountAllInACell*”. Fig. 4

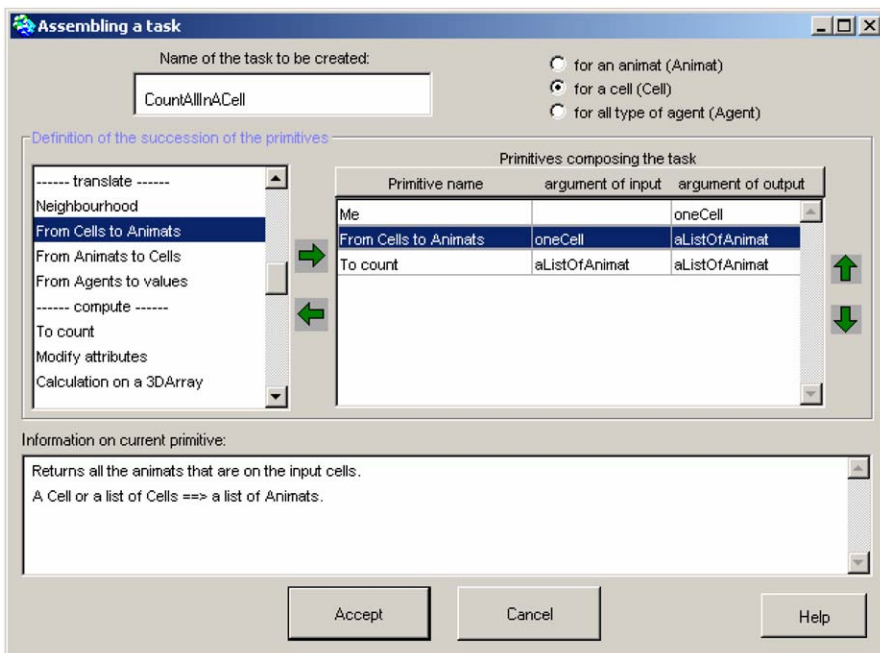


Fig. 4. Example of building a task “*CountAllInACell*” with primitives. The linear sequence of the different stages of a task (locate → sort → compute → update) and the different classes of primitives provided by MobidyC are detailed in [11]. Primitives exchange only one argument: starting with the current cell, the translate primitive “*From Cells to Animats*” returns all animats in the cell. Finally the compute primitive “*To count*” stores in a attribute of the cell (here a list type attribute) the number of animats.

shows an example of building the task “*CounAllInACell*” composed of three primitives: a find type primitive (“*Me*”), a translate primitive (“*From Cells to Animats*”) and a compute type primitive (“*To count*”). The component programming and the use of primitives within “*Mobidyc*” platform are detailed in [11].

#### 4. Describing space-time multi-scale patterns of simulated populations

A key issue in ecological science is to understand how a population occupies the available physical space as a whole, but also how patches of different intensity are spatially organized in order to infer e.g. how long a limited resource can sustain a population. This is addressed here using related but conceptually different analysis methods to investigate the spatial structure of the simulated population of *E. affinis*. The simulated population clearly presents a differential spatial structure when observed for simulation times ranging from 10 to 60 days (Fig. 5). In particular, apart from the obvious fluctuations in abundance, the population appears rather inhomogeneously distributed over the simulation domain, and presents different levels of intermittency. We analyse below this inhomogeneity and its time evolution using several scaling analysis techniques. We first show the non-uniform and non-Gaussian character of abundance values using rank-frequency analysis and considering the probability density of the field. Next we consider the degree of space-filling of the population and its time evolution. We then focus on the multiple-scaling properties of the abundance field, using several multifractal analysis techniques.

##### 4.1. The total population distribution in each cell

We consider first an analysis of the intensity distribution in the peaks visible in Fig. 5. This is done here without considering spatial information, for the  $128 \times 128$  cells simulation, hence presenting 3584 values for an estimate of the distribution of the total population in each cell.

A first approach corresponds to a rank-ordering approach, also called “Zipf plot”. This corresponds to the observation of the frequency of occurrence of any event, as a function of the rank  $r$ , when the rank is determined by the above frequency of occurrence. Zipf’s law [40] corresponds to a power-law rank-ordering curve: the frequency  $f_r$  of the  $r$ th largest occurrence of the event is inversely proportional to its rank  $r$  as  $f_r = f_1/r$  where  $f_1$  is the frequency of the most frequent (i.e. the largest) event in the distribution. In log–log scales, the Zipf distribution gives a straight line with slope  $-1$ . The generalized Zipf distribution is subsequently defined as  $f_r = f_1/r^\alpha$  where the log–log plot can be linear with any slope  $\alpha$ . More generally, the Zipf law can be written as

$$X_r \propto r^{-\alpha}, \quad (1)$$

where  $X_r$  is the “*weight*” of an occurrence of an event relative to its rank  $r$ , and  $\alpha = 1$  and  $\alpha \neq 1$  for the Zipf’s and the generalized Zipf’s law, respectively. Alternatively, a “uniform” behaviour will manifest itself as a continuous roll-off from a horizontal line (i.e.  $\alpha \rightarrow 0$ ) to a vertical line (i.e.  $\alpha \rightarrow \infty$ ). This is representative of the fact that every value (bounded between a minimum and a maximum) is equiprobable. In addition, we

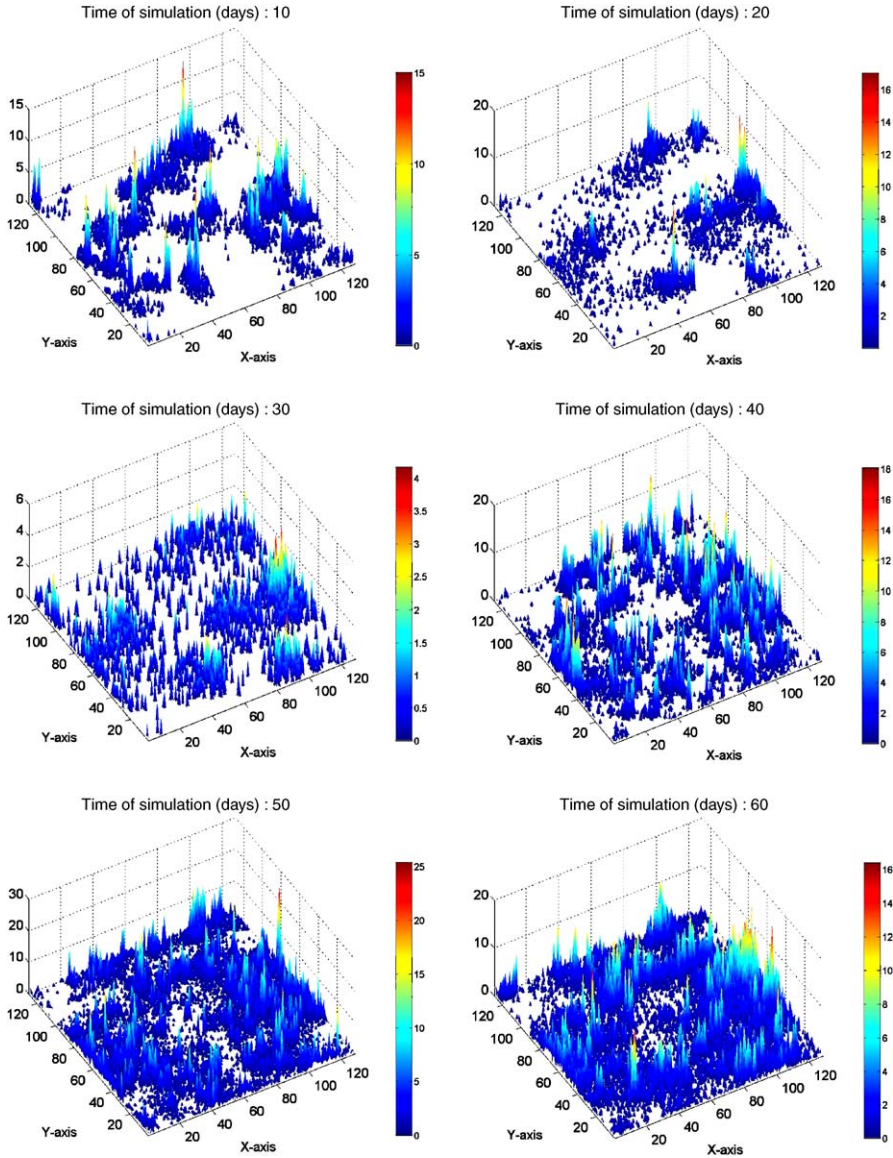


Fig. 5. Spatio-temporal development of the total population of the copepod *Eurytemora affinis* simulated in spatial grid  $128 \times 128$ . Only time of simulation multiple of 10 days are selected.

stress that this framework can be directly applied to discrete processes (e.g. zooplankton abundance), as well as continuous processes (e.g. phytoplankton concentration) through Eq. (1). Applying Eq. (1) to the simulated population on a  $128 \times 128$  cells illustrates the above stated arguments. The Zipf curves, shown for simulation times of 10, 30 and 60

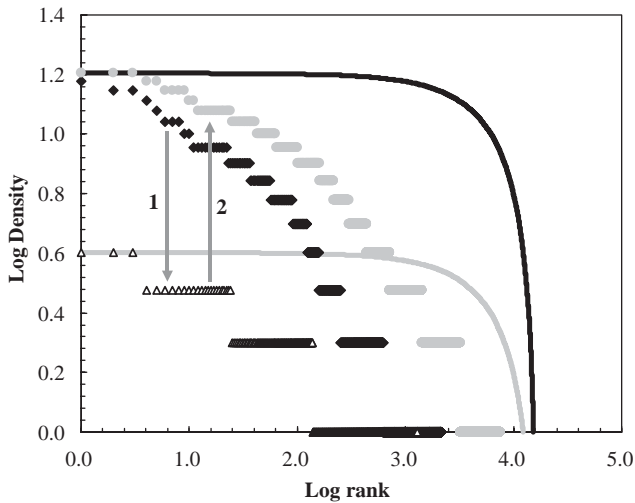


Fig. 6. Illustration of the non-uniform character of the distribution of the simulation of a population of the copepod *Eurytemora affinis* after 10 days (diamonds), 30 days (triangles) and 60 days (grey dots) of simulation. The continuous curves represent simulated uniform distributions with the same minimum and maximum values of densities than the observed populations after 10 days (grey curve) and 60 days (black curve). The size of the spatial grid is  $128 \times 128$  cells.

days, are compared with the curves expected in case of uniform distributions with the same minimum and maximum values than the simulated ones (Fig. 6). It appears that even if the empirical curves cannot be reasonably fitted by a linear regression, they nevertheless clearly exhibit more structures than the uniform distributions. In addition, the Zipf curves exhibit a “hysteresis-like” effect associated to the massive mortality (principally the remaining adults) observed after 30 days of simulation (see Fig. 6). After 10 days of simulation, the statistical distribution of the simulated population is then similar to the one observed after 60 days of simulation, even if their simulated spatial distributions are clearly different (Fig. 5). The lack of structure observed in the population after 30 days of simulation stems from the very weak observed abundance (i.e. ranging from 1 to 4 individuals per cell).

The rank-ordering approach gives in fact access to the same information as the probability distribution, but presented in another manner. This consists mainly in considering the cumulative distribution (see [31] for a comparative discussion). We consider here also the probability density of the total population for times 40, 50 and 60 (Fig. 7). A Gaussian probability density function (pdf) with the same mean and variance as the population at time 60, is shown for comparison. It is clear that the population distribution per cell is quite far from a Gaussian distribution, since large events are much more frequent. Furthermore, at the times considered, the pdf have roughly the same behaviour: in a log-linear plot, the curves are not far from each other, and rather nicely fitted by a stretched exponential of equation  $Ce^{-ax^\beta}$ , where  $C = 0.53$  and  $a = 1.5$  are constants and  $\beta = 0.6$  is the characteristic exponent of the stretched exponential ( $\beta = 2$  for Gaussian variables,  $\beta < 1$  for fat-tailed distributions, see discussions in [31]).

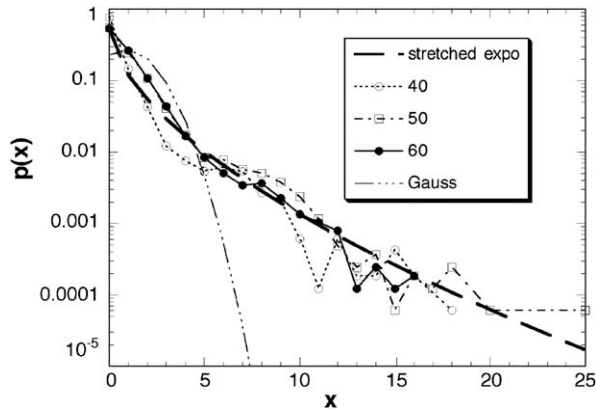


Fig. 7. Probability density function of the total population in each cell, for a grid of  $128 \times 128$  cells, and for time steps 40 (open triangles), 50 (open squares) and 60 (black dots). A Gaussian probability density function (pdf) is shown for comparison, having the same mean and variance as the experimental population at time 60. A better fit is provided by a stretched exponential (thick dotted line).

These close but complimentary analyses showed that the distribution of the total population per cell is not uniform nor Gaussian, and presents a specific variability that can be relatively nicely fitted by a stretched exponential with fat-tailed probability distribution function.

#### 4.2. Fractal presence-absence of the population and its time evolution

The degree of space-filling of *E. affinis* population is investigated via its scaling (i.e. fractal) properties. Knowing that a fractal dimension of a set characterizes its space-filling properties (see e.g. Feder, 1988), on a two-dimensional space a uniform set of points will then have a higher fractal dimension than less homogeneously distributed point patterns (Fig. 8). To estimate the fractal dimension of *E. affinis* population, we first binarized its distribution (Fig. 9) such as each cell containing at least one individual is blackened. The initial distributions (see Fig. 5) are now transformed into point patterns (Fig. 9). A practical method to estimate the fractal dimension is to superimpose a regular grid of pixels of length  $\lambda$  on the object, and count the number of “occupied” pixels. This procedure is repeated using different values of  $\lambda$ . The surface occupied by a point pattern is then estimated with a series of counting boxes spanning a range of volumes down to some small fraction of the entire volume. The number of occupied boxes increases with decreasing box size, leading to the following power-law relationship:

$$N(\lambda) \propto \lambda^{-D}, \quad (2)$$

where  $\lambda$  is the box size,  $N(\lambda)$  is the number of boxes occupied by the path and  $D$  the fractal dimension.  $D$  is estimated from the slope of the linear trend of the log–log plot of  $N(\lambda)$  versus  $\lambda$ . Fig. 10 illustrates the application of the previous fractal analysis to the point patterns estimated from the  $128 \times 128$  cells simulations. The linearity of the log–log plot of

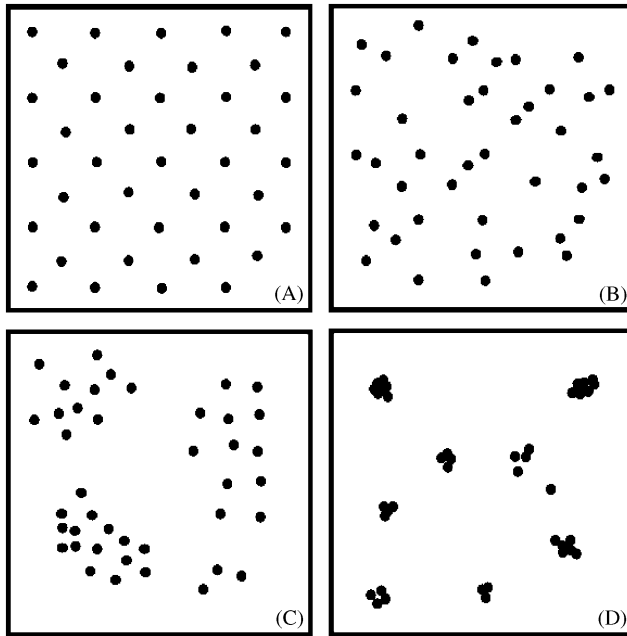


Fig. 8. Schematic illustration of the concept of fractal dimension. A regular point pattern (A) will have a higher fractal dimension than a “random” point pattern (B), a random clumped point pattern (C) and an aggregated clumped point pattern (D).

$N(\lambda)$  vs.  $\lambda$  is very good (Fig. 10A) and demonstrates the emergence of scaling properties from our model of the population dynamics of the copepod *E. affinis*. The subsequent time course of the fractal dimensions estimated from simulated patterns of simulation times ranging from 2.5 to 60 days (with 2.5 days increments) is shown in Fig. 10B. The space-filling character of *E. affinis* total population increases rapidly until a critical threshold of  $D = 1.5$  is reached after a simulation time of 10 days. The fractal dimension then decreases until a minimum is reached at simulation time of 32.5 days. The population finally increases its space-filling character up to a maximum dimension of  $D = 1.87$ . It seems that the space-filling properties of the total population are here under a density-dependent control as the decrease and increase observed in the fractal dimensions (Fig. 10B) occur, respectively, while the total abundance of the population decreases and increases (see Figs. 3 and 5).

#### 4.3. Multi-scaling properties of the total population repartition

The next issue addressed here is to know whether the patches of different abundance are similarly distributed in space. Eq. (2) can be modified as

$$N_\lambda(C > c) \propto \delta^{-D_i}, \quad (3)$$

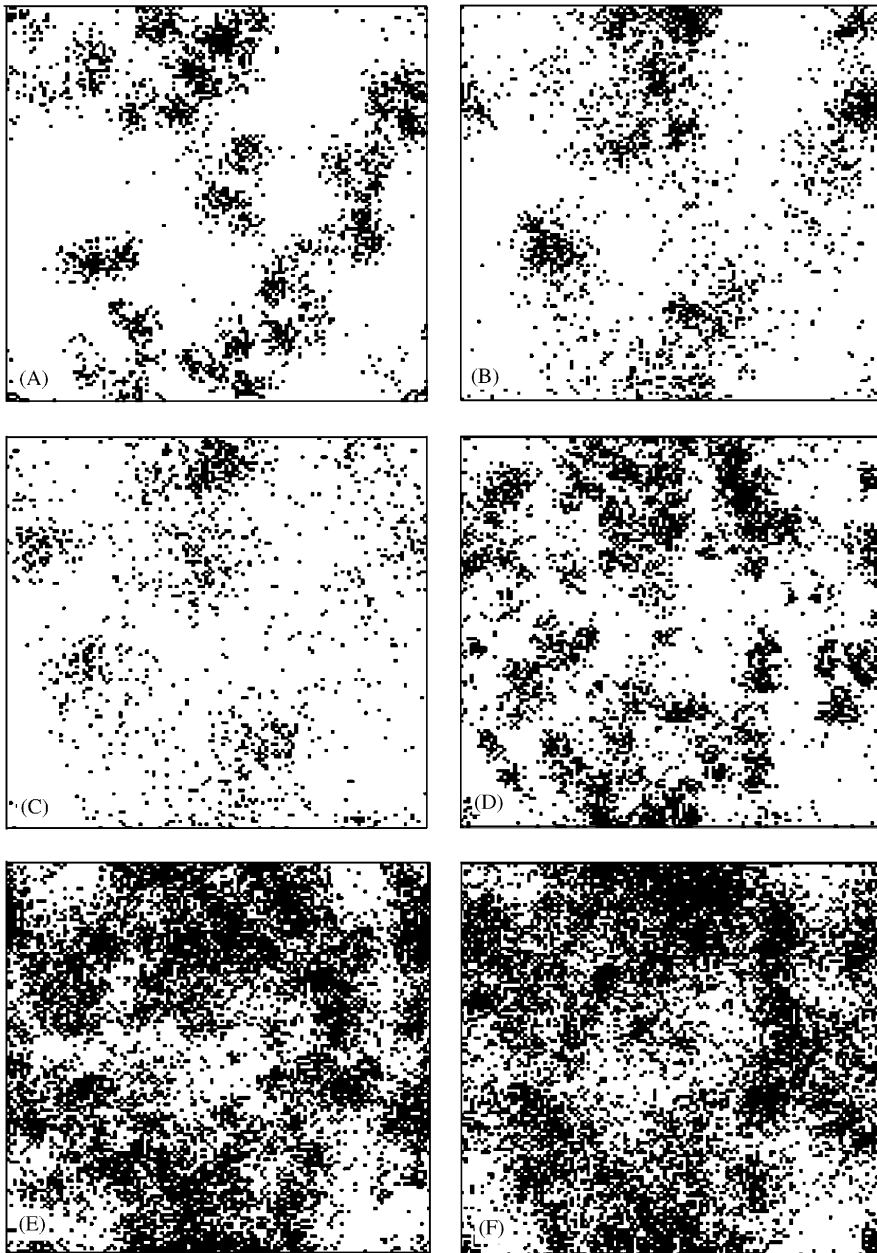


Fig. 9. Binary illustration of the spatio-temporal development pattern of the total population of a simulation of the copepod *Eurytemora affinis* in spatial grid  $128 \times 128$  cells. The occupied cells are black. The size of the spatial grid is  $128 \times 128$  cells. The different panels (A–F) correspond to the increasing times of simulation shown in Fig. 5 (10–60 days).

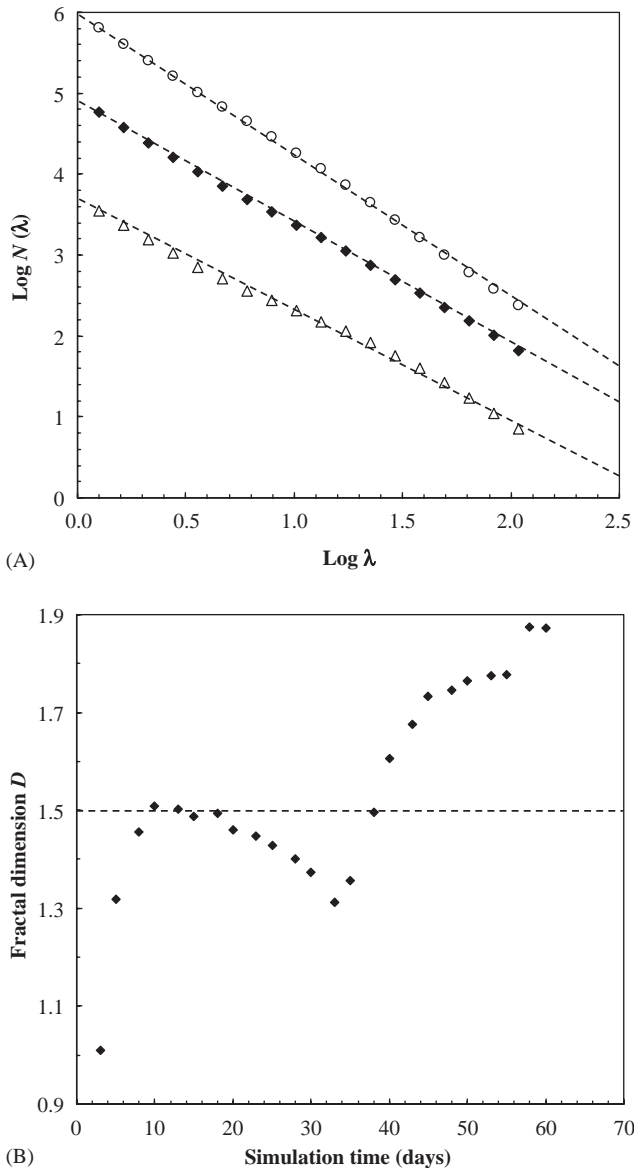


Fig. 10. Illustration of the scaling behaviour of the point patterns of *Eurytemora affinis* population after 10 days (diamonds), 30 days (triangles) and 60 days (open circles) of simulation (A), and the time course of the fractal dimensions estimated for simulation times ranging from 2.5 to 60 days with 2.5 days increments (B). The size of the spatial grid is  $128 \times 128$  cells.

where  $N_\lambda(C > c)$  corresponds to the number of boxes of length  $\lambda$  containing more individuals than a threshold value  $c$ , and  $D_i$  the multifractal function associated to the threshold value  $c$ . For each threshold concentration  $c$ , the slope of the log–log plot of  $N_\lambda(C > c)$

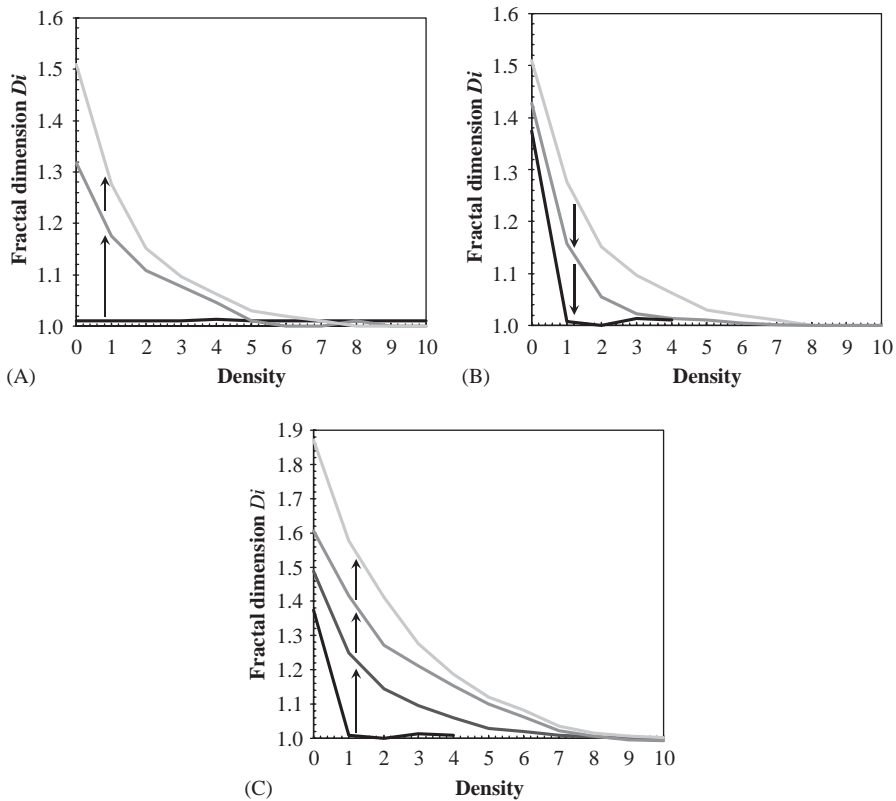


Fig. 11. Time course of the multifractal functions  $D_i$ , estimated for three sets of simulations time: (A) 2.5, 5 and 10 days (from bottom to top), (B) 10, 20 and 30 days (from top to bottom), and (C) 30, 37.5, 40 and 60 days (from bottom to top). The size of the spatial grid is  $128 \times 128$  cells.

vs.  $\lambda$  is an estimate of  $D_i$ ; each threshold value  $c$  is thus characterized by its own fractal dimension. In particular, the nonlinearity of the function  $D_i$  when plotted against the threshold value  $c$  is indicative of multifractality. The shape of the function  $D_i$  then provides an estimate of the level of complexity of the spatial structure in a given population. A very fast decrease of  $D_i$  towards a minimum value of 1 will then characterize a population dominated by a low-density background where high-density patches are very heterogeneously distributed and basically reduced to a few aggregated clumped point pattern (see Fig. 8). On the opposite, the slower the  $D_i$  decrease is, the more space filling is the distribution of high-density patches, and the more complex is the whole structure of the population. This is illustrated by the time course of the estimated function  $D_i$  (Fig. 11). As previously suggested, the structure of the population presents a density-dependent “hysteresis-like” effect. The complexity of the population spatial structure then increases with simulation times up to 10 days (Fig. 11A), then decreases with the decrease in abundance for simulation times ranging from 10 to 30 days (Fig. 11B). Finally, the complexity of the population spatial structure increases again from simulation times ranging from 30 to 60 days (Fig. 11C).

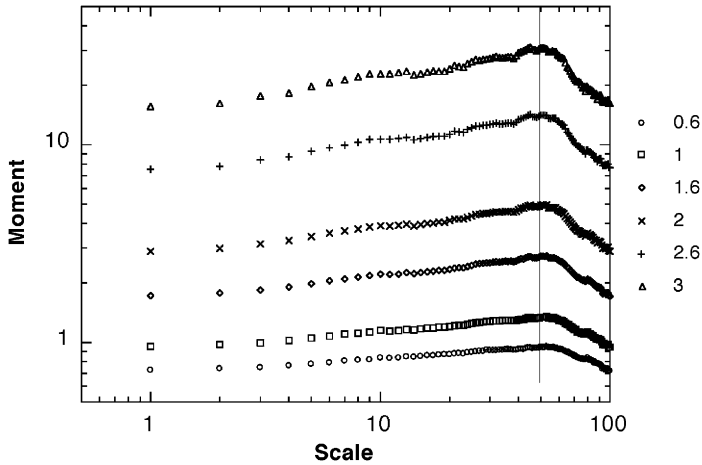


Fig. 12. Scaling invariance of the total density field, for a grid of  $128 \times 128$  and at time 60. Moments vs. distances for the shears are represented (from bottom to top, moments of order 0.6, 1, 1.6, 2, 2.6, 3. A clear scaling regime is visible, for scales up to about 60. This upper bound for the scaling regime corresponds to half the radius of the grid.

Another way to consider the multi-scale properties of the structures is to introduce an analysis technique coming from the field of turbulence (see [25,9]), and aiming at studying the moments of order  $q > 0$  of the amplitude of the difference  $\Delta X_l = \|X(M) - X(N)\|$  of the field  $X$  between position  $M$  and position  $N$ , which is assumed here (hypothesis of isotropy and stationarity of increments) to depend only on the distance  $l = d(M, N)$  between the two positions. For an isotropic 2D multifractal field, we thus expect, as an analogy with turbulent properties (see [30,29] for applications of multifractal structure functions to plankton populations):

$$\langle \Delta X_l^q \rangle \approx l^{\zeta(q)}, \tag{4}$$

where  $\langle \cdot \rangle$  means ensemble average and  $\zeta(q)$  is a scale invariant function (a second characteristic function, in the field of probability theory) which is nonlinear and concave, and characterizes the scaling properties of the fluctuating field  $X$ . In particular, for a fractal (often called in this case “monofractal”) field,  $\zeta(q)$  is linear; for example for a Brownian motion  $\zeta(q) = q/2$ , and for a fractional Brownian motion of index  $H$ ,  $\zeta(q) = qH$ . The moment approach is useful to characterize the whole hierarchy of fluctuations, since low-order moments (close to 0) characterize weak fluctuations, while larger order moments (in practice up to moments of order 4) characterize larger fluctuations. Let us also recall that the moments of order 1 and 2 correspond to the mean and variance of the fluctuations, a framework which is generalized here since we consider a continuous range of values of  $q > 0$ .

This procedure is applied to the  $128 \times 128$  grid, at time 60, showing the most variability, and for which the multiple-scaling analysis is the more likely to be justified. The structure functions are shown in Fig. 12, giving the moment order versus the scale (distance between

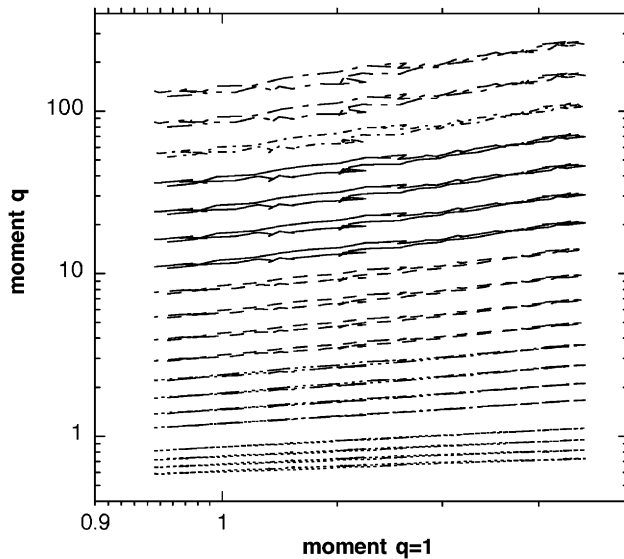


Fig. 13. Application of the extended self-similarity (ESS) technique, for moments from 0.2 to 4 (from bottom to top). This consists in plotting the moment of order  $q$  vs. the moment of order 1, in log–log representation.

points), for various orders of moments. The scaling of Eq. (4) is well verified up to a scale of about 60, which is closer to half the size of the grid (128): this is expected since the simulation are done on a torus, so that the maximum reachable distance between two points is half the dimension of the grid. For more accurate estimation of the slopes, a variant of the structure function plot is applied, which is also coming from the field of turbulence: this is called extended self-similarity (ESS) [3], and consists in representing  $\langle \Delta X_l^q \rangle$  vs.  $\langle \Delta X_l \rangle$  (instead of  $\langle \Delta X_l^q \rangle$  vs.  $l$ ). This writes

$$\langle \Delta X_l^q \rangle \approx \langle \Delta X_l \rangle^{z(q)} \tag{5}$$

when Eq. (4) is verified, Eq. (5) will give  $z(q) = \zeta(q)/\zeta(1)$ . Both approaches will then give formally the same result, but in practice, as shown originally by Benzi et al. [3], the self-similar scaling given by Eq. (5) is much more accurate than the scaling present in Eq. (4). This general property has been shown to be present in many fields, and we show in Fig. 13 that this is also the case for our simulation:  $z(q)$  is estimated for a whole range of moments orders, and since  $H = 0.1$  may be estimated separately, this provides an accurate estimation of the function  $\zeta(q)$ , shown in Fig. 14. This figure confirms the weak multifractality of the data:  $H$  is relatively small and the experimental curve departs from linear behaviour (corresponding to homogeneous fractal) only for moments larger than 3. Nevertheless, it is an interesting property since it shows that simple rules may generate heterogeneous multifractal properties for the total zooplankton spatial distribution. Such properties were already observed in the field for zooplankton distribution [26,29]. In the latter case, however, the multifractality is more pronounced, certainly due to the effect of turbulence, while in the present simulation, turbulence is of course absent.

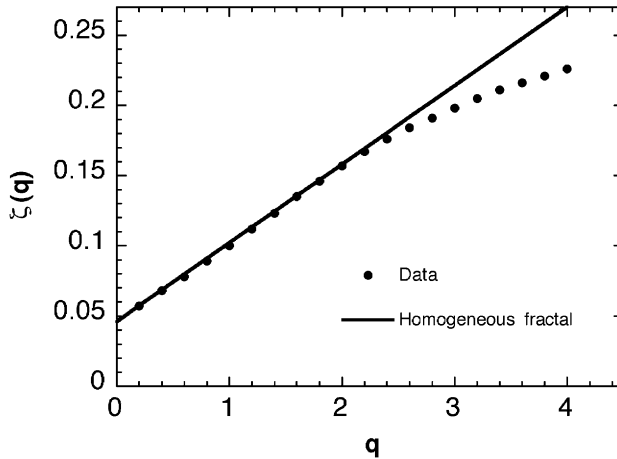


Fig. 14. The scaling moment function characterizing the scale-invariant fluctuations of the total density field (black dots), for grid  $128 \times 128$  at time 60. This function is slightly nonlinear, showing a slight—but nevertheless clear—multifractal property. The line corresponding to an homogeneous fractal is shown for comparison (continuous line).

## 5. Discussion

### 5.1. Individual-based models and theoretical frameworks

The increasing importance of individual-based modelling over the last decade has resulted in an exponential increase in the number of papers using these techniques in the field of ecology. The IBMs are constructed using a “bottom-up” approach by detailing the dynamics of entities making up the system and their interactions. However, this recent popularity of IBMs may hamper progress without reaching a consensus on how these models should be developed. IBMs can easily reach high complexity levels, making their description or their readability very difficult. One fundamental difficulty in the evaluation and comparison of IBMs in the literature comes from the lack of any theoretical formalism, such as differential equations, where one can express, conserve and compare one model to another, or to export it to another modelling tool. The development of IBMs in both terrestrial and aquatic ecosystems contributed in some extent to improve our understanding of the complexity of interactions and organization of natural systems. Grimm [12] considered that a unified theory has not yet emerged from IBMs developed in the 1990s. At the beginning of IBMs development, modellers did not explicitly address the question of how they should link theories in ecology with their models. The differences in motivations (studied ecosystem, main questions and goals) and modelling tools may justify why modellers spent more time in developing their models (use of complex computer programming i.e. object-oriented languages and software engineering) rather than analysing them in a more general theoretical framework. However, these simulation models generally lead to very complex computer programs, which are extremely prone to bugs [15]. These difficulties explained the gap between the early development of IBMs and the general theory of ecological systems. This

handicap is now partially overcome by the recent development of simulators and dedicated tools making IBMs more accessible to all ecologists [20,11]. More recently, Grimm and Railsback [14] suggested the development of an individual-based theory and explained how population dynamics emerge from individual traits and interactions.

With the proposed tools it is possible to focus on applications with the general objective of analysing the emerging properties of the model. In the present context the main properties of the model are its multi-scale heterogeneity, coming from the fact that birth is clustered while death occurs randomly in space. This non-symmetric birth–death process, associated to a normal diffusion, generates heterogeneous distributions, even if all the processes and exchanges between individuals are purely local and memory less. To obtain a wilder heterogeneity, and clear long-range correlations between abundances, other rules should be introduced, possessing e.g. non-local influences on birth and death processes, or “wilder” movements PDFs. Such “experimental” and numerical exploration, considering the spatial and temporal correlations, and the multi-scale heterogeneities in association with the type of rule for birth, death and movements, is clearly possible with the present platform. It can provide new insights in the generation of multi-scale patchiness, through the identification of universal emerging properties in space and time.

## 5.2. Use of dedicated tools and platforms: application to copepod population model

In this paper a recently proposed platform called Mobidyc dedicated to end-users is used to develop the copepod population model and also the different scenarios of simulations. The principles and the architecture of this platform, based on multi-agents systems (MAS), are detailed in Ginot et al. [11]. The encoding effort is concentrated at the level of the different tasks that the agent has to execute, or at the even more elementary level called “primitives”, at which the previous tasks may be broken down into. An example of using of these primitives to make a task “*CountAllInACell*” was shown in Fig. 4. This approach facilitates the conception of models, restricts programming errors and increases readability. The example of the population dynamics of the estuarine copepod *E. affinis* evolving at constant and optimal temperature (15 °C) was chosen for the following practical reasons: (i) the population cannot be modelled by a single stage because of the characteristics of life cycle of copepods; (ii) only the last stage (adult) can reproduce; (iii) several experimental and empirical studies focused on this species of copepods; and, (iv) the results of the recently developed individual-based experiments for studying (in the laboratory) life cycle characteristics of this species [6] allowed to correctly parameterize the demographic processes used in the model (i.e. mean stage duration and its variability). The high number of stages used in the model increases the number of demographic processes (tasks) and parameters (attributes). Theoretically, the modification of any parameter value (or a combination of parameters) could result in a modification of the simulated patterns. Such sensitivity analysis is out of the scope of our paper. The main objective is to show for the first time the high potential of using scaling and multi-scaling techniques for analysing the generated patterns by spatially explicit IBMs in ecology. For these reasons, the mean probabilities of survival in all stages as well as egg production for females are considered constant. In addition no density-dependent effect was introduced in the model. In other words the obtained spatial and temporal patterns are solely generated by the random walk of individuals at local scale

and the other demographic processes (birth, metamorphosis and mortality) in the absence of any externally imposed pattern. For this particular case the model can be simplified by lumping naupliar stages (N1–N6) and the first copepodite stages (C1–C4). But for more realistic conditions where the heterogeneity of stage-specific probabilities of survival is a general rule, the lumping of developmental stages may engender errors when the average parameters are estimated [32]. However, in practice the end-user define one developmental stage (i.e. egg), then Mobidyic platform offers the possibility of duplication of this agent. The user can easily update the state of the new agent (stage) and if necessary add the adequate new tasks (i.e. two moulting tasks in C4). The only possible limitation is the size of the spatial grid and/or the total number of the active agents during the simulation. This is a classic limitation of most IBMs that require powerful computers. In our examples a personal computer (Pentium IV; 3.02 Ghz and 1 Go RAM) was used to run all simulations. The simulations with  $128 \times 128$  cells and a 6 hours time step took less than 2 days.

### 5.3. *Emerging space-time properties in zooplankton populations*

Young et al. [39] showed that the population of very simple random walking organisms developing in a homogeneous environment can lead to the emergence of spatial patterns. However, in their model the reproduction is simply represented by binary division and the mortality rate is considered constant. In our example we tried to develop more realistic life representation of a planktonic organism by including discrete developmental stages. The development from one stage to another and the survival were represented stochastically. In order to understand the combined effects of demographic processes (at the population level) and the local behaviour (random walk) on the emerging patterns the parameterization of the model was kept as simple as possible. Although these simplistic assumptions were used in the model, the generated patterns showed significant scaling and multi-scaling properties. This is a first and immediate objective reached by this study. For future studies the quantification of these patterns using the same techniques or other techniques may allow analysing the complexity of the behaviour of these IBMs. One can envisage testing the effect of modifying the basic behaviour of individuals (i.e. aggregative behaviour) or the introduction of spatially heterogeneous resources. The last example is easy to implement with Mobidyic because each cell is an agent and can exhibit a simple or more complex dynamics. The user can also use ascii files to fill the space in either the initial conditions or for each time step. The space-time patterns generated by the model developed here to describe the population dynamics of the estuarine copepod *E. affinis* can be regarded as being realistic as on the basis of a very simple parameterization of the life cycle of this species they exhibited several properties that have been previously observed in the field for zooplankton populations. These properties are (i) non-uniformity, (ii) scale-dependence (or fractal behaviour), and (iii) intermittent (or multifractal) behaviour. In addition, we stress here that these properties are fully compatible with those observed in the field for phytoplankton and zooplankton populations (e.g. [26,30,29,21]), ensuring the relevance of the emerging simulated patterns. On this basis, it is reasonable to think that the inclusion of critical biological parameters such as behaviour, cannibalism and predation, and physical parameters as ubiquitous as advective and turbulent processes should improve the realism of the model, as well as the convergence between its emerging fractal and multifractal properties and the fractal and

multifractal properties of in situ populations. Several theoretical studies showed the inclusion of 2D spatial representation of very simple predator–prey or host–parasitoid models (i.e. Lotka–Volterra) can generate complex spatio-temporal patterns [5,28].

#### 5.4. Effects of the size of the simulation domain

We finally stress that the size of the grids used to conduct the simulations is potentially a critical, while often neglected, limitation of the IBMs that can have significant effect on the properties of the simulated population. Schofield et al. [28] used initial conditions of 100 hosts distributed randomly through a domain ( $25 \times 25$  cells) in ten patches, each containing ten hosts. Then all their subsequent simulations and analyses were based on the same domain and the same initial conditions. In another domain (medical) Mansury et al. [23] used an agent-based model to study the emerging patterns in tumour systems. They used a  $48 \times 48$  cells for all analyses. In these examples (and others) the size of the grids was not discussed, however, we believe that this issue is interesting and the sensitivity of the patterns to the size of the spatial domain should be discussed. This is already done in

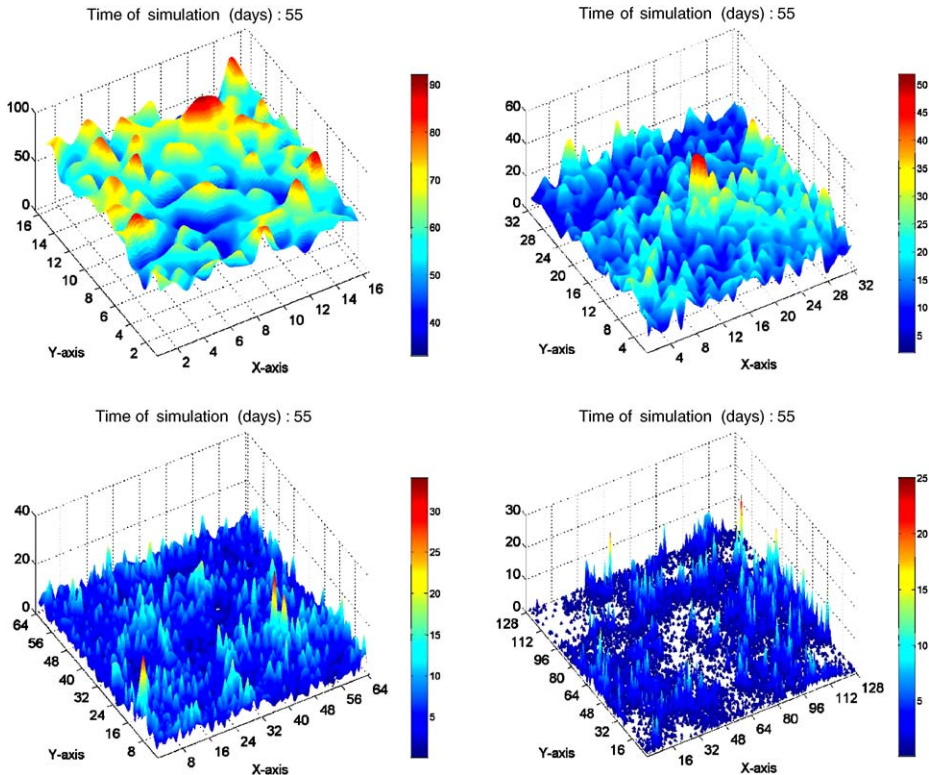


Fig. 15. Spatial distribution of the total population of the copepod *Eurytemora affinis* after 55 days of simulation in four sizes of spatial grids:  $16 \times 16$ ,  $32 \times 32$ ,  $64 \times 64$  and  $128 \times 128$  cells.

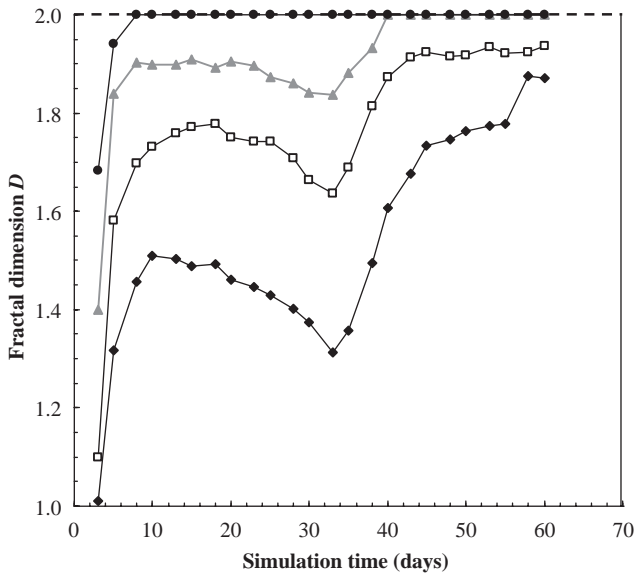


Fig. 16. The time course of the fractal dimensions estimated for simulation times ranging from 2.5 to 60 days (with 2.5 days increments) for four sizes of spatial grids:  $16 \times 16$  pixels (black dots),  $32 \times 32$  (grey triangles),  $64 \times 64$  (open squares) and  $128 \times 128$  cells (black diamonds).

other numerical fields such as turbulence modelling, where the effect of the grid on turbulent profiles is systematically studied [37]. To illustrate this issue in our study, one must compare the differences perceptible in the distribution of the total abundance of *E. affinis* when the same model is ran on grids of different sizes (Fig. 15). First, it appears that for a given simulation time (here 55 days), the total number of individuals is highly dependent on the size of the grid (Fig. 15). Second, the visual appearance of the distribution is also very distinct between each simulation; as for instance the intermittency of the distribution sharply increases with the size of the domain. Finally, we investigate the space-filling properties of each of these distributions for simulation times ranging from 2.5 to 60 days (Fig. 16). For grid sizes of  $32 \times 32$ ,  $64 \times 64$  and  $128 \times 128$  cells, the time course of the related fractal dimensions exhibits roughly similar and consistent behaviours. However, in case of  $16 \times 16$  cells grid the population is space filling after a simulation time of 7.5 days (Fig. 16). As this could have critical consequences, for instance in case of a study aimed at estimating how a limited resource can sustain the growth and survival of a grazing populations, this issue should systematically be critically and carefully addressed before using any IBM to infer ecologically relevant situation.

## Acknowledgements

The MOBIDYC platform (version 2.1) is freely available in French, English, and German and a tutorial (in French and English) is provided. It uses the Smalltalk Visual Works 7 envi-

ronment developed by the Cincom Company. This environment is free for non-commercial use and runs on almost all platforms: <http://www.avignon.inra.fr/mobidyc>. This project aims to create a network group, which can participate in the improvement and development of these tools and also enrich the library of models. The models developed here can be downloaded (or obtained from S.S.) and immediately used. This paper is a contribution to the Programme Seine-Aval II. We thank David Devreker and Gael Dur for their contribution in the estimation of the parameters of copepod model.

## References

- [1] E.R. Abraham, The generation of plankton patchiness by turbulent stirring, *Nature* 391 (1998) 577–580.
- [2] C.M. Andersen, T.G. Nielsen, Hatching rate of the egg-carrying estuarine copepod *Eurytemora affinis*, *Mar. Ecol. Prog. Ser.* 160 (1997) 283–289.
- [3] R. Benzi, S. Ciliberto, R. Tripiccone, C. Baudet, G. Ruiz Chavarria, Extended self-similarity in the dissipation range of fully developed turbulence, *Europhys. Lett.* 24 (1993) 275–279.
- [4] L. Berec, Techniques of spatially explicit individual-based models: construction, simulation, and mean-field analysis, *Ecol. Model.* 150 (2002) 55–81.
- [5] D. Coca, S.A. Billings, Identification of coupled map lattice models of complex spatio-temporal patterns, *Phys. Lett. A* 287 (2001) 65–73.
- [6] D. Devreker, S. Souissi, L. Seuront, Effects of individual variability on the development and mortality of the first naupliar stages of *Eurytemora affinis* (Copepoda, Calanoida) under different conditions of salinity and temperature, *J. Exp. Mar. Biol. Ecol.* 303 (2004) 31–46.
- [7] L. Fahse, C. Wissel, V. Grimm, Reconciling classical and individual-based approaches in theoretical population ecology: a protocol for extracting population parameters from individual-based models, *Am. Nat.* 152 (1998) 838–852.
- [8] C.L. Folt, C.W. Burns, Biological drivers of plankton patchiness, *TREE* 14 (1999) 300–305.
- [9] U. Frisch, *Turbulence, the Legacy of A.N. Kolmogorov*, Cambridge University Press, London, 1995.
- [10] S. Gasparini, J. Castel, X. Irigoien, Impact of suspended particulate matter on egg production of the estuarine copepod, *Eurytemora affinis*, *J. Mar. Systems* 22 (1999) 195–205.
- [11] V. Ginot, C. Le Page, S. Souissi, A multi-agents architecture to enhance enduser individual based modelling, *Ecol. Model.* 157 (2002) 23–41.
- [12] V. Grimm, Ten years of individual-based modelling in ecology: what have we learned and what could we learn in the future?, *Ecol. Model.* 115 (1999) 129–148.
- [13] V. Grimm, U. Berger, Seeing the forest for the trees, and vice versa: pattern-oriented ecological modelling, in: L. Seuront, P. Strutton (Eds.), *Handbook of Scaling Methods in Aquatic Ecology: Measurement, Analysis, Simulation*, CRC Press, Boca Raton, 2004, pp. 411–428.
- [14] V. Grimm, S.F. Railsback, *Individual-Based Modelling and Ecology*, Princeton University Press, Princeton, NJ, 2005 (in press).
- [15] V. Grimm, T. Wyszomirski, D. Aikman, J. Uchmanski, Individual-based modelling and ecological theory: synthesis of a workshop, *Ecol. Model.* 115 (1999) 275–282.
- [16] A.R. Hough, E. Naylor, Endogenous rhythms of circatidal swimming activity in the estuarine copepod *Eurytemora affinis* (Poppe), *J. Exp. Mar. Biol. Ecol.* 161 (1992) 27–32.
- [17] H.I. Jager, Individual variation in life history characteristics can influence extinction risk, *Ecol. Model.* 144 (2001) 61–76.
- [18] A. La Barbera, B. Spagnolo, Spatio-temporal patterns in population dynamics, *Physica A* 314 (2002) 120–124.
- [19] A. Lomnicki, Population ecology from the individual perspective, in: L.J. Gross (Ed.), *Individual-Based Models and Approaches in Ecology*, Chapman & Hall, New York, 1992, pp. 3–17.
- [20] H. Lorek, M. Sonnenschein, Modelling and simulation software to support individual-based ecological modelling, *Ecol. Model.* 115 (1999) 199–216.

- [21] S. Lovejoy, W.J.S. Currie, Y. Teissier, M.R. Claereboudt, E. Bourget, J.C. Roff, D. Schertzer, Universal multifractals and ocean patchiness: phytoplankton, physical fields and coastal heterogeneity, *J. Plankton Res.* 23 (2001) 117–141.
- [22] D.L. Mackas, K.L. Denman, M.R. Abbott, Plankton patchiness: biology in the physical vernacular, *Bull. Mar. Sci.* 37 (1985) 652–674.
- [23] Y. Mansury, M. Kimura, J. Lobo, T.S. Diesboeck, Emerging patterns in tumor systems: simulating the dynamics of multicellular clusters with an agent-based spatial agglomeration model, *J. Theoret. Biol.* 219 (2002) 343–370.
- [24] H. Minar, R. Burkhart, C. Langton, M. Askenazi, The swarm simulation system: a toolkit for building multiagent simulations, Working Paper 96-06-042, Santa Fe Institute, 1996.
- [25] A.S. Monin, A.M. Yaglom, *Statistical Fluid Mechanics: Mechanics of Turbulence*, MIT Press, Cambridge, 1975.
- [26] M. Pascual, F.A. Ascoti, H. Caswell, Intermittency in the plankton: a multifractal analysis of zooplankton biomass variability, *J. Plankton Res.* 17 (1995) 1209–1232.
- [27] S.F. Railsback, Concepts from complex adaptive systems as a framework for individual-based modelling, *Ecol. Model.* 139 (2001) 47–62.
- [28] P. Schofield, M. Chaplain, S. Hubbard, Mathematical modelling of host parasitoid systems: effects of chemically mediated parasitoid foraging strategies on within- and between-generation spatio-temporal dynamics, *J. Theoret. Biol.* 214 (2002) 31–47.
- [29] L. Seuront, Y. Lagadeuc, Multiscale patchiness of the calanoid copepod *Temora longicornis* in a turbulent coastal sea, *J. Plankton Res.* 23 (2001) 1137–1145.
- [30] L. Seuront, F.G. Schmitt, Y. Lagadeuc, D. Schertzer, S. Lovejoy, Universal multifractal analysis as a tool to characterise multi-scale intermittent patterns; example of phytoplankton distribution in turbulent coastal waters, *J. Plankton Res.* 21 (1999) 877–922.
- [31] D. Sornette, *Critical Phenomena in Natural Sciences: Chaos, Fractals, Selforganization and Disorder: Concepts and Tools*, Springer, New York, 2000.
- [32] S. Souissi, S. Ban, The consequences of individual variability in moulting probability and the aggregation of stages for modelling copepod population dynamics, *J. Plankton Res.* 23 (2001) 1279–1296.
- [33] S. Souissi, V. Ginot, L. Seuront, S.-I. Uye, Using multi-agent systems to develop individual based models for copepods: consequences of individual behaviour and spatial heterogeneity on the emerging properties at the population scale, in: L. Seuront, P. Strutton (Eds.), *Handbook of Scaling Methods in Aquatic Ecology: Measurement, Analysis, Simulation*, CRC Press, Boca Raton, 2004, pp. 527–546.
- [34] D.J. Sumpter, D.S. Broomhead, Relating individual behaviour to population dynamics, *Proc. R. Soc. London B* 268 (2001) 925–932.
- [35] A. Tsuda, H. Sugisaki, T. Ishimaru, T. Saino, T. Sato, White-noise-like distribution of the oceanic copepod *Neocalanus cristatus* in the subarctic North Pacific, *Mar. Ecol. Prog. Ser.* 97 (1993) 39–46.
- [36] J. Uchmanski, V. Grimm, Individual-based modelling in ecology: what makes the difference?, *TREE* 11 (1996) 437–441.
- [37] D.C. Wilcox, *Turbulence Modelling for Computational Fluid Dynamics*, DCW Industries, 1998.
- [38] W.G. Wilson, Lotka's game in predator–prey theory: linking populations to individuals, *Theor. Popul. Biol.* 50 (1996) 368–393.
- [39] W.R. Young, A.J. Roberts, G. Stuhne, Reproductive pair correlations and the clustering of organisms, *Nature* 412 (2001) 328–331.
- [40] G.K. Zipf, *Selective Studies and the Principle of Relative Frequency in Language*, Harvard University Press, Cambridge, 1932.